This is a repository copy of *Computational modelling of interactions between gold complexes and silicates*.

White Rose Research Online URL for this paper:
http://eprints.whiterose.ac.uk/112045/

Version: Accepted Version

Article:

Accepted Manuscript

Computational Modelling of Interactions between Gold Complexes and Silicates

Sima Mohammadnejad, John L. Provis, Jannie S.J. van Deventer

Please cite this article as: S. Mohammadnejad, J.L. Provis, J.S.J. van Deventer, Computational Modelling of Interactions between Gold Complexes and Silicates, *Computational & Theoretical Chemistry* (2016), doi: http://dx.doi.org/10.1016/j.comptc.2016.12.036

Computational Modelling of Interactions between Gold Complexes and Silicates

Sima Mohammadnejad,[1,2] John L. Provis*[2,3], Jannie S.J. van Deventer[2]

[1] Department of Mining, Tarbiat Modares University, P.O. Box 14115-143, Tehran, Iran

[2] Department of Chemical and Biomolecular Engineering, The University of Melbourne, Victoria 3010, Australia

[3] Department of Materials Science and Engineering, University of Sheffield, Sheffield S1 3JD, UK.

* corresponding author; current address: Email j.provis@sheffield.ac.uk, phone +44 114 222 5490

Abstract

The interactions of gold complexes including gold chloro-hydroxy species, gold thiosulphate and gold thiourea, with protonated and deprotonated silicate monomers, are studied using density functional theory (DFT) methods. The previously published optimal geometry of gold complexes is used here, together with the geometry of silica monomers that is optimised and compared with experimental and available theoretical data. COSMO (COnductor like Screening Model) solvation simulation of different systems (for different pH and gold complexes) is also used to represent the surrounding aqueous environments. The interaction energy of gold complexes with silica species based on theoretical studies has been shown to correlate well with the extent of silica preg-robbing (sorption) per surface area of quartz determined experimentally. The ability of DFT to compute the interactions of different gold complexes involving significant relativistic effects, with other species, has been demonstrated in this study. This work allows us to explain and control the chemical processes which result in loss of gold from solution in hydrometallurgical extraction.

Keywords: Density functional theory; COSMO solvation; gold chloride; gold thiourea; gold thiosulphate; silicate

1. INTRODUCTION

Carbonaceous matter and sulphides are well known to adsorb gold from leaching solutions in a phenomenon known as preg-robbing [1]. The mechanism of interaction of gold complexes with ore constituents has been the subject of investigation over the last few decades [2], and it has more recently been demonstrated that silicates can also be highly problematic in causing preg-robbing. However, previous studies of preg-robbing have focused mainly on gold cyanide complexes in view of its dominant use in gold extraction, meaning that non-cyanide gold complexes have not received as much attention. With increasing community resistance to the use of cyanide, there is renewed

interest in alternative lixiviants in both research and industry. The interaction of non-cyanide gold complexes including chloride, thiourea and thiosulphate in contact with framework (quartz and feldspar) and layer silicates (kaolinite and pyrophyllite) were studied experimentally in our group [3-8]. A significant preg-robbing effect was observed in most of the systems, contradicting previously held beliefs.

The interaction of Au(I) and Au(III) complexes with other species was studied for the first time by Tossell [9] in the presence of sulphide and chloride, at the Hartree–Fock (HF) level with limited solvent effects. Becker and co-workers [10] used density functional theory (DFT) methods to calculate the adsorption energy of gold chloride (in $AuCl_4^-$ form) on the surface of galena. However, no details of the geometrical characterisation of gold complexes were presented in that study.

Several studies have been conducted in the last decade on the interaction of non-cyanide gold complexes with other species including silanols and silicates. Hong and co-workers [11, 12], following their extensive experimental studies on the interaction of gold complexes with kaolinite, also used some computational methods. The results of their quantum mechanics calculations using the SCF-Xα-DV (self-consistent-field discrete-variation method) method revealed that the edge sites of kaolinite dominate the complexation reactions of the kaolinite surface with AuS^- and $Au(HS)_2^-$ anions, especially at sites near the Al octahedra. Wojtaszek [13, 14] et al. also investigated the interaction of gold particles with a silica surface using periodic DFT. Their results show that the sorption strength of gold on silica decreases with increasing chloride concentration at the surface, with increasing cluster size, and with decreasing oxidation state of gold. The most stable grafting complex was shown to be $AuCl(OH)_3^-$ on a chloride-free silica surface, while the presence of Si-Cl groups at the surface destabilises the complex.

There is a significant lack of knowledge available in the literature regarding computational characterisation of non-cyanide gold complexes and their interaction with other species including silicates. Most of the studies available are limited to gas phase calculation or a low level of computational theory due to the high atomic number of gold and associated high computational costs, which are particularly introduced by relativistic effects.

Here, we have applied high level computational modelling and implicit solvent models to study the interaction of different complexes with silica monomers at different pH conditions, comparable with the experimental conditions published in our previous work.

2. COMPUTATIONAL METHODS

Density functional modelling has been carried out using the software DMol[3], implemented in Accelrys Materials Studio version 4.4 (Accelrys, San Diego, USA). The most stable and optimised geometry of each gold complex, as published previously [15], is used in this study, while the geometry of silica monomers is optimised and compared with experimental and available theoretical data. The simulations were implemented using generalised gradient functionals as described below, running on a Quad-core desktop PC.

A double numerical basis set was used (two atomic orbitals for each occupied orbital) for all atoms plus a p-function polarisation on all hydrogen atoms (DNP) to account for hydrogen bonding [16]. In our previous study [15], a series of calculations were performed to assess the performance of the different exchange-correlation functionals as well as orbital cut off values; from this assessment PBE functionals and a 10 Å orbital cut off were applied [15]. No pseudo-potentials or effective core potentials were used in this study and all the results are based on "All Electron Relativistic" calculations.

The continuum solvation model, (COnductor like Screening MOdel, COSMO) [13] and the dielectric constant of water (78.54) were used to describe both acidic and alkaline solutions of the different gold complexes in the dilute solutions studied here. Multipolar expansion was used for calculation of the solvation energy for all molecules except OH^-, for which a monopolar expansion was used. Geometry optimisation convergence thresholds were set at 1×10^{-6} hartrees, 2×10^{-4} hartrees/Å and 5×10^{-4} Å for energy, maximum force and maximum displacement respectively. An SCF convergence of 10^{-7} hartrees was used with no smearing, with an orbital cut off of 10 Å for all types of atoms.

The interaction energy of species has been calculated based on the difference between the SCF energy of combined complexes and individual molecules ($E_{Si\ monomer+Gold\ Complex} - E_{Si\ monomer} - E_{Gold\ Complex}$) in kcal·mol^{-1}.

3. RESULTS AND DISCUSSION

3.1.   GOLD COMPLEXES

Speciation of gold chloro-hydroxy species, as well as gold thiourea and thiosulphate, has been reported by our group [15]. The same geometrical data have been used in this study.

3.2.   SILICA SPECIES

Silica has an equilibrium solubility in aqueous solution of ~100 ppm (~2 mM) at near-neutral pH at around 25 °C [17], and the most stable form of silica in aqueous solutions over a wide range of pH (approximately 2-10) is silicic acid, $Si(OH)_4$. Above this concentration, silicic acid undergoes condensation or polymerisation, reducing the silicic acid concentration to its equilibrium solubility and generating stable polynuclear species [18]. The concentration of Si is very low in the aqueous leaching systems studied here (<10 ppm for framework silicates as well as acidic clays), so dimerisation or polymerisation products of silica have not been considered in this study.

Hydrolysis and deprotonation of the silicate monomer have been studied extensively [18-20]. At a pH below 2, which is the point of zero net charge of silica, protonation of silanols forms cationic species $[Si(OH)_n(OH_2)_{4-n}]^{(4-n)+}$ (n < 4) [19]. Above pH 10, further hydrolysis involves the deprotonation of a silanol group to form an anionic species:

$$[Si(OH)_{4-n}O_n]^{n-} \rightarrow [Si(OH)_{(3-n)}O_{n+1}]^{(n+1)-} + H^+ \qquad , 0 \leq n \leq 3 \qquad \text{(Equation 1)}$$

Because $Si(OH)_3O^-$ is the conjugate base of a weak acid, it is observed only in appreciable quantities above pH 12 [19, 20], and the second deprotonation requires even more highly alkaline conditions. Figure 1 demonstrates the dominant silica monomer species over the pH ranges from 0-14.
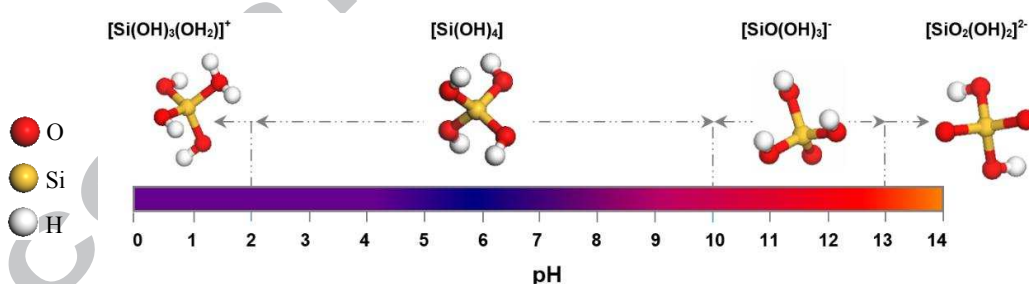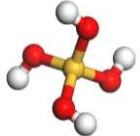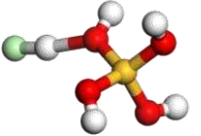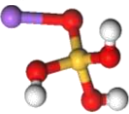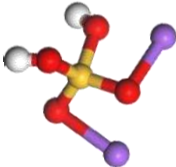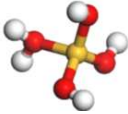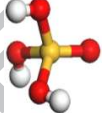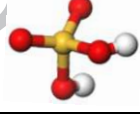

Figure 1. Hydrolysis and deprotonation of silica monomers at different pH.

The structures of the possible silicate monomers (neutral; singly charged cation and anion; doubly charged anion), considering the realistic pH values used in our experiments, were modelled in this work. To enable simulation of neutral species, enough Na^+ ions were added to charge-balance the anions $Si(OH)_3O^-$ and $Si(OH)_2O_2^{2-}$, and Cl^- to charge-balance the cation $Si(OH)_3(OH_2)^+$. The optimised geometries in the gas phase and COSMO for all the structures are presented in Tables 1 and 2.

4
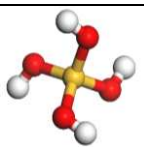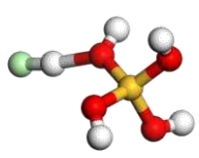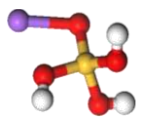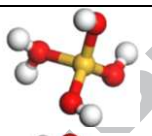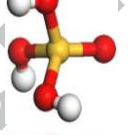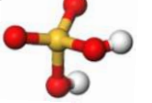
Table 1. The optimised geometries and thermochemical parameters of silica monomers in the gas phase. ⬤ Cl ⬤ : O ⬤ : H ⬤ : Si ⬤ : Na
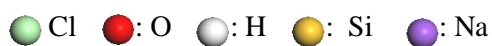
Silica monomers	Si-O bond length (Å)	O-Si-O bond angle (°)	Binding energy (kcal·mol^{-1})
Neutral monomers			
[Si(OH)$_4$]	1.65	106	-903.6
Neutral models for charged monomers			
[Si(OH)$_3$OH$_2$Cl]	Si-OH: 1.65, 1.64, 1.64 Si-OH$_2$Cl: 1.66	111,112, 113,114	-1041.3
[Si(OH)$_3$ONa]	Si-OH: 1.67, 1.67, 1.73 Si-ONa: 1.58	101,103, 103,116	-907.1
[Si(OH)$_2$O$_2$Na$_2$]	Si-OH: 1.70, 1.75 Si-ONa: 1.59,1.64	118,113, 99,100	-881.1
Charged monomers			
[SiOH$_2$(OH)$_3$]$^+$	Si-OH: 1.60, 1.61, 1.61 Si-OH$_2$: 1.85	93,103, 113,121	-804.8
[SiO(OH)$_3$]$^-$	Si-OH: 1.57, 1.70, 1.70 Si-O: 1.72	100,100, 112,114	-888.3
[SiO$_2$(OH)$_3$]$^{2-}$	Si-OH: 1.79 1.79, Si-O: 1.59,1.62	102,102, 110,110	-723.3

Table 2. The optimised geometries and thermochemical parameters of silica monomers in COSMO.

○: Cl ●: O ○: H ●: Si ●: Na

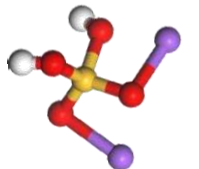| Silica monomers	Bond length (Å)	Bond Angle (°)	Binding Energy (kcal·mol⁻¹)
Neutral monomers			
[Si(OH)₄]	1.65	115	-944.1
Neutral models for charged monomers			
[Si(OH)₃OH₂Cl]	Si-OH: 1.64, 1.64, 1.65, Si-OH₂Cl: 1.67	100,107, 113,116	-1058.5
[Si(OH)₃ONa]	Si-OH: 1.67, 1.67, 1.73 Si-ONa: 1.58	103,104, 110,119	-933.4
[Si(OH)₂O₂Na₂]	Si-OH: 1.70, 1.73 Si-ONa: 1.60,1.62	104,104, 114,115	-917.9
Charged monomers			
[SiOH₂(OH)₃]⁺	Si-OH: 1.61, 1.62, 1.62 Si-OH₂: 1.79	103, 104, 114, 119	-876.8
[SiO(OH)₃]⁻	Si-OH: 1.69, 1.69, 1.70, Si-O: 1.57	102, 107, 112, 118,	-961.5
[SiO₂(OH)₃]²⁻	Si-OH:1.75, 1.75, Si-O: 1.60, 1.60	102, 107, 108, 123	-961.3

To validate the structures of different silicate monomer species, the Gibbs free energies were calculated for deprotonation reactions of silica monomers, and the results were compared with experimental and theoretical data reported in the literature in Table 3. The description of the aqueous phase in each of the calculations was based on the COSMO model, and explicit water molecules were not included. As is depicted in the third equation in Table 3 for each type of species, some literature studies have used four explicit water molecules in the protonated form and three water molecules in neutral and deprotonated forms, to improve the simulation of the solution chemistry via

theoretical methods [21], but in the current work this was not found to be beneficial as the inclusion of explicit water molecules greatly extended the computational demands (time and memory) of the calculations involving also gold complexes.

Table 3. Values of stability constant ($\log_{10}\beta$) of protonation and deprotonation of $Si(OH)_4$ monomer.

Reaction	Theo.	Exp.	This work
$[Si(OH)_3(OH_2)]^+ + OH^- \rightarrow Si(OH)_4 + H_2O$	4.7[a]		4.4
$[Si(OH)_3(OH_2)]Cl \rightarrow Si(OH)_4 + HCl$	0.2[a]		1.8
$[Si(OH)_3(OH_2)]^+ \cdot 4H_2O + OH^- \rightarrow Si(OH)_4 \cdot 4H_2O + H_2O$	3.0[b]		
$Si(OH)_4 + OH^- \rightarrow SiO(OH)_3^- + H_2O$	-7.3[a]	-9.5[c]	-13.6
$Si(OH)_4 + NaOH \rightarrow NaSiO(OH)_3 + H_2O$	-8.6[b]		-10.1
$Si(OH)_4 \cdot 3H_2O + NaOH \rightarrow NaSiO(OH)_3 \cdot 3H_2O + H_2O$	-5.1[b]		
$SiO(OH)_3^- + NaOH \rightarrow SiO_2(OH)_2^{2-} + H_2O$	0.4[b]	-3.2[d], -4.0[e]	0.2
$NaSiO(OH)_3 + NaOH \rightarrow Na_2SiO_2(OH)_2 + H_2O$	-7.6[b],		-9.5
$NaSiO(OH)_3 \cdot 3H_2O + NaOH \rightarrow Na_2SiO_2(OH)_2 \cdot 3H_2O + H_2O$	-3.0[b,]		

Literature sources:

a: [22] - HF and DFT

b: [21] -DFT

c: [23]

d: [24]

e: [18]

The deprotonation reactions were simulated here using both OH^- and sodium hydroxide (NaOH) as the basic reactants, where in each case the hydroxide ion (OH^-) forms water through extraction of a hydrogen ion (H^+) from the silicate monomer.

The protonation and deprotonation energies of silica monomers at 298 K have been reported in the literature using different theoretical and experimental techniques (Table 3). Considering the fact that the best theoretical results reported in the literature are based on consideration of at least three explicit water molecules, while none were taken into account here, the results show reasonable correlation with both experiments and previous theoretical data. The use of neutral models for the charged silicates results in better correlation with experiments (-10.1 vs. -13.6 for 1st deprotonation). Unfortunately there are no experimental data available in the literature regarding protonation of $Si(OH)_4$, however the data obtained here without explicit water molecules are relatively close to the results reported by Tossell and Sahai [22] including explicit water molecules.

Although there is some level of discrepancies between the calculated values of stability constants from these theoretical studies and the available experimental data, the optimised geometries for the silica monomer could be still used for investigation of interaction with gold complexes via trend analysis of interaction energies.

3.3. INTERACTION OF GOLD COMPLEXES WITH SILICA SPECIES

Our previous experimental studies showed a considerable interaction between silicate solids and dissolved species with different gold complexes [7]. The key aim of this study is to examine these interactions at a molecular level using DFT methods. The gold species and silicate monomers were simulated as described above. To obtain results which can be used in comparison with experimental data, we need to look at the interactions across the wide range of pH conditions used in experiments. Table 4 lists the pH ranges used in the experiments, which correspond to the pH ranges used in industrial scale gold leaching systems.

Table 4. pH values of experimental systems.

Gold complex	pH	
	Acidic	Alkaline
Chloro-hydroxide	2-3	8-8.5
Thiourea	1.5	12-12.5
Thiosulphate		9.5

As discussed above, gold chloride species undergo dechlorination and silica monomers undergo deprotonation at higher pH values. However, gold thiourea and gold thiosulphate can each only form one stable complex. Here, the interactions of different gold chloro-hydroxy complexes with silicates were studied systematically as a function of the number of chloride ligands, as well as gold thiourea and thiosulphate. The interaction energies of all of the different gold complexes with $Si(OH)_3(OH_2)^+$, $Si(OH)_4$ and $Si(OH)_3O^-$ were examined and these trends were used to predict the interaction behaviour even where stability of each particular species is improbable. For silica monomers, charged species were used for interaction studies to avoid possible interactions between charge balancing ions (Na^+ or Cl^-) in the neutral species which might not be present in the real systems.

3.3.1. Chloride Systems

The optimised geometries of different gold chloro-hydroxy species with silica monomers, along with interaction energies in gas and COSMO models, are shown in Figure 2. $Si(OH)_4$ is the dominant monomer across pH 2-10, where all five different gold chloro-hydroxy species could be stable. At very high pH, the silica monomer is deprotonated as presented in Figure 1, however $Au(OH)_4^-$ is also reduced to metallic gold. Also, pH values less than 2 or greater than 9, where protonation and deprotonation of $Si(OH)_4$ occur respectively, are out of the experimental ranges and have not been considered for simulation.

The form of gold chloro-hydroxy species at low pH (0-3.5) is $Au(Cl)_4^-$. The adsorption of this form by a neutral silica monomer (also representing an uncharged surface) is significantly less likely. For the completely chlorinated form of the species, the only possible interaction is $Au-Cl\cdots HO-Si$, which seems to be repulsive as it results in a positive free energy of interaction in COSMO (10.7 kcal·mol^{-1}). To determine the role of surrounding media in this interaction, the free energy of adsorption in the gas phase was also calculated (Figure 2). This reaction is slightly favourable in the gas phase, however it still shows the lowest tendency towards interaction compared with the other species studied. The low adsorption energy between gold chloride ($AuCl_4^-$) and the deprotonated form of silica cluster ($Si(OH)_4$) suggests a low gold uptake by the quartz surface, which contradicts the experimental data [7], where all of the silicates evaluated, especially quartz and pyrophyllite, showed strong adsorption at pH 2-2.5. This pH is very close to the zero charge point of silica and on the verge of protonation/deprotonation, so the existence of protonated silica sites, represented in simulations by the protonated form of the silica monomer $Si(OH)_3(OH_2)^+$, is likely. Therefore, for this monomer the interaction of the protonated silica monomer with $AuCl_4^-$ was also considered. As expected, a much higher interaction energy results from these two oppositely-charged ions, -92.8 kcal·mol^{-1} in gas and 1.7 kcal·mol^{-1} in COSMO media. The optimised geometry for the $Si(OH)_3(OH_2)^+\ldots AuCl_4^-$ interaction is presented in Figure 3, along with a plot of the interaction energy for this reaction. It has to be noted that in the computational modelling conducted by Wojtaszek [13] the same silica surface properties were considered for all species, whereas in reality silanol groups change protonation state as a function of pH, which can result in differences in sorption behaviour as presented here.
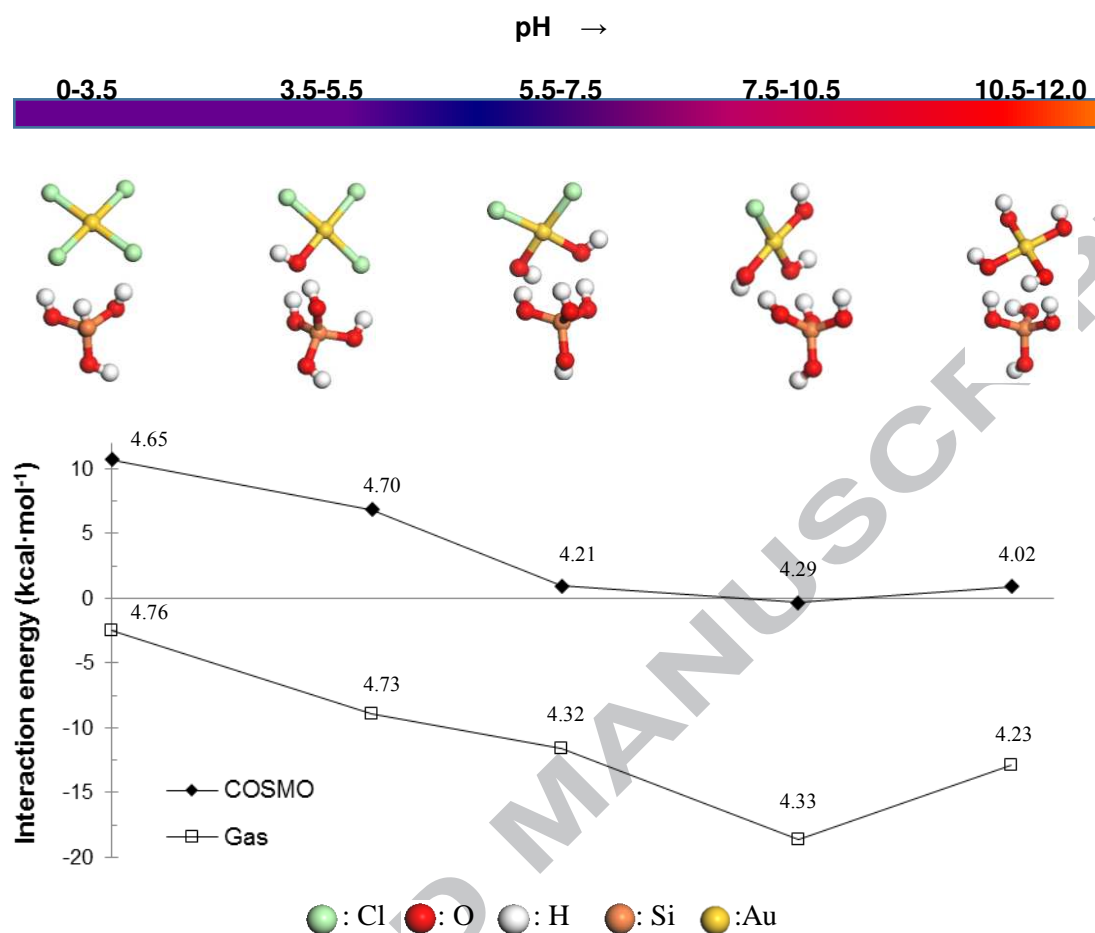
Figure 2. Optimised geometries of gold chloro-hydroxy species interacting with $Si(OH)_4$ in COSMO and interaction energies in both gas and COSMO. The values accompanying each data point show the Au-Si distance in Å. In the molecular graphics, light green is Cl, red is O, white is H, orange is Si, and dark yellow is Au.

The dechlorination of gold chloro-hydroxy species makes the interaction significantly less unfavourable. However, the interaction energy is still positive for the next two species, $AuCl_3(OH)^-$ (pH 3.5-5.5) and $AuCl_2(OH)_2^-$ (pH 5.5-7.5). The free energy decreases by about 4 kcal·mol^{-1} in the first stage of dechlorination, and a further 6 kcal·mol^{-1} in the second dechlorination to $AuCl_2(OH)_2^-$. This result indicates that the Au-OH…OH-Si interaction is attractive, in contrast with Au-Cl…OH-Si. The hydrogen bonding between the H atom of one molecule and the OH group of the other molecule results in an attractive force between the two molecules.
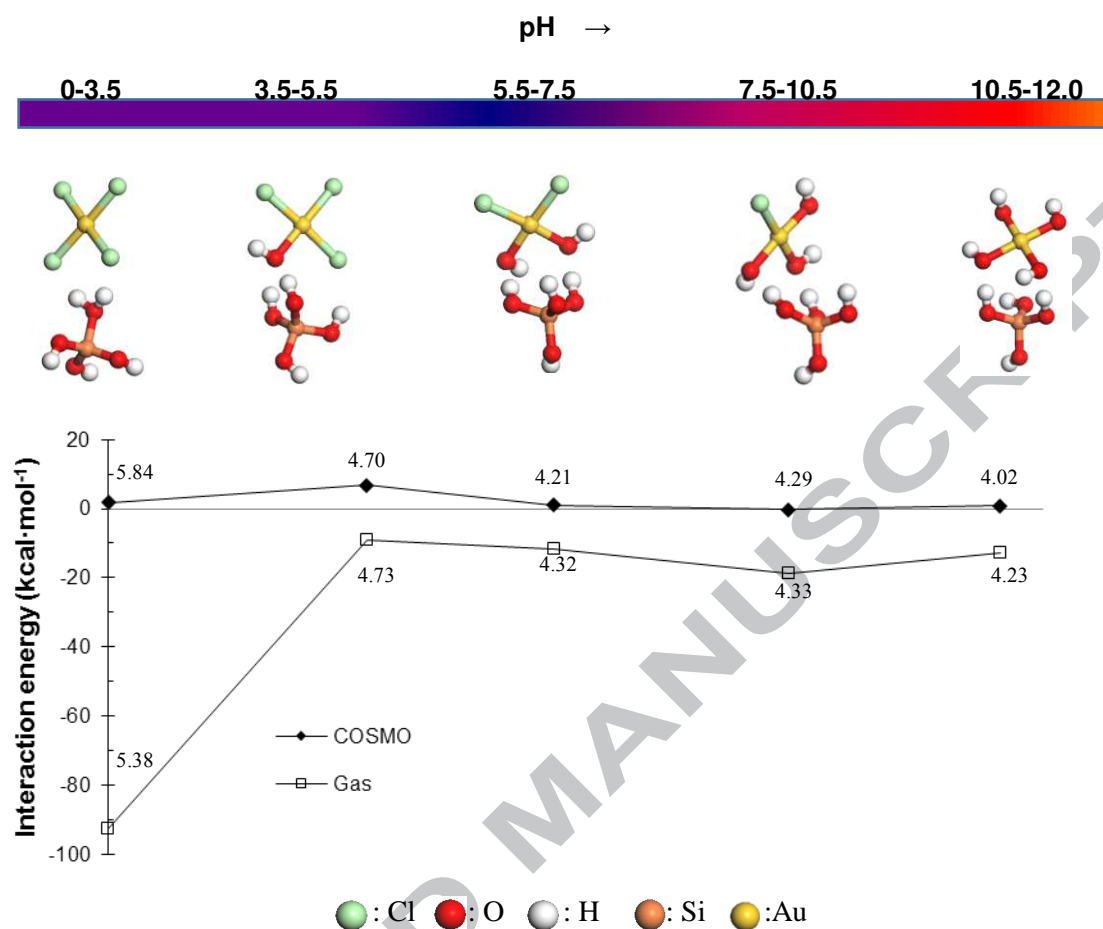
Figure 3. Optimised geometries of $AuCl_{4-n}(OH)_n$ interacting with $Si(OH)_3(OH)_2^+$ for n = 0 and $Si(OH)_4$ for n = 1-4 in COSMO, and interaction energies in both gas and COSMO. The values on each data point show the Au-Si distance in Å.

Increasing the OH content further, $AuCl(OH)_3^-$ (pH 7.5-9) yields a minimum in interaction energy. This species is the only one studied which has a favourable interaction with the neutral silica monomer. However, it is interesting that further replacement of Cl with OH groups at pH 9-14 does not increase the strength of the interaction, but rather shifts the reaction to be slightly unfavourable, very similar to $AuCl_2(OH)_2^-$. This result is in agreement with both the experimental and theoretical results of Wojtaszek [13], who reported the highest interaction of the mesoporous silica surface with this $AuCl(OH)_3^-$ form of the gold chloro-hydroxy complex. The optimum pH for production of gold-containing silica-supported catalysts has also been found to be around 9 [25]. The experimental observation of the amount of gold uptake by quartz at pH 8-8.5 [7] also reveals significant adsorption of the $AuCl(OH)_3^-$ species (0.03-0.09 μmol.m^{-2}). However, the reduced adsorption for the case of $Au(OH)_4^-$, where the highest amount of adsorption would be expected, is not yet explained.

Thus, it is necessary to introduce another effect which plays a significant role determining the interaction between these two molecules. It is proposed that the geometry of these two species, specifically the square planar structure of gold chloro-hydroxy species and the tetrahedral structure of silica monomer, is of great importance. Wojtaszek [13] stated that four interactions including repulsive interactions of Au-Cl…OH-Si groups, and attractive interactions of Au-OH…OH-Si, are present where gold chloro-hydroxy species are interacting with silanol groups. However, we believe that due to geometry constraints (enforced by the original bonding of Si-OH in silanol groups and Au-Cl or Au-OH in gold chloro-hydroxy species), not all of the ligands are contributing to the adsorption, and this is clear from the geometries of the optimised interacting complexes.

In $AuCl_4^-$, the H atoms of two of the OH groups in the silica monomer are aligned with the Cl ligands of the gold complex. In $AuCl_3(OH)^-$, it seems that only one Au-OH…OH-Si interaction is contributing to the reaction process, and all three other ligands (repulsive) are not notably aligned or repositioned in the presence of the other molecule. For the next two species, $AuCl_2(OH)_2^-$ and $AuCl(OH)_3^-$, two ligands are contributing, with more effect in the former as there is less repulsive force due to Cl groups. However, in the fully dechlorinated form, three OH groups are involved, in the absence of Cl groups on the gold atom, and this results in some distortion of both molecules. In the most stable geometry of $Au(OH)_4^-$ (Tables 1 and 2), the OH groups are all aligned. However, the optimised geometry of $Au(OH)_4^-$-$Si(OH)_4$ (Figure 3) illustrates that the OH groups are significantly re-arranged in interaction with the silica cluster to give a geometry close to conformer number 12 in Table 3 of [15], which is about 1.4 kcal·mol^{-1} less stable than the most stable conformer of that species. In all other gold chloro-hydroxy species, the optimised geometry in the presence of the silica cluster is almost identical to the most stable form of the isolated structure. It is suggested that this reorganisation of the original molecular geometries plays an important role in the lower adsorption of gold on silicates at high pH values (9-14).

In conclusion, the interaction of the gold chloro-hydroxy species with $Si(OH)_4$ is unfavourable, except for $AuCl(OH)_3^-$ which is slightly favourable. The trend in gold adsorption by silicates as a function of pH is dominated by Au-OH· · ·OH-Si attractive and Au-Cl · · ·OH-Si repulsive interactions. The respective geometries of the square planar gold chloro-hydroxy species and the tetrahedral silica monomer limit the total number of contributing ligands, which contributes to the maximum in the case of $AuCl(OH)_3^-$.

3.3.2. Thiourea System

The interaction of gold thiourea cations with all three different type of silica monomers $Si(OH)_4$, $SiO(OH)_3^-$ and $Si(OH)_3(OH_2)^+$ was investigated in both gas and COSMO phase. The optimised geometries as well as interaction energies are presented in Figure 4. The optimised geometries presented are based on COSMO models.
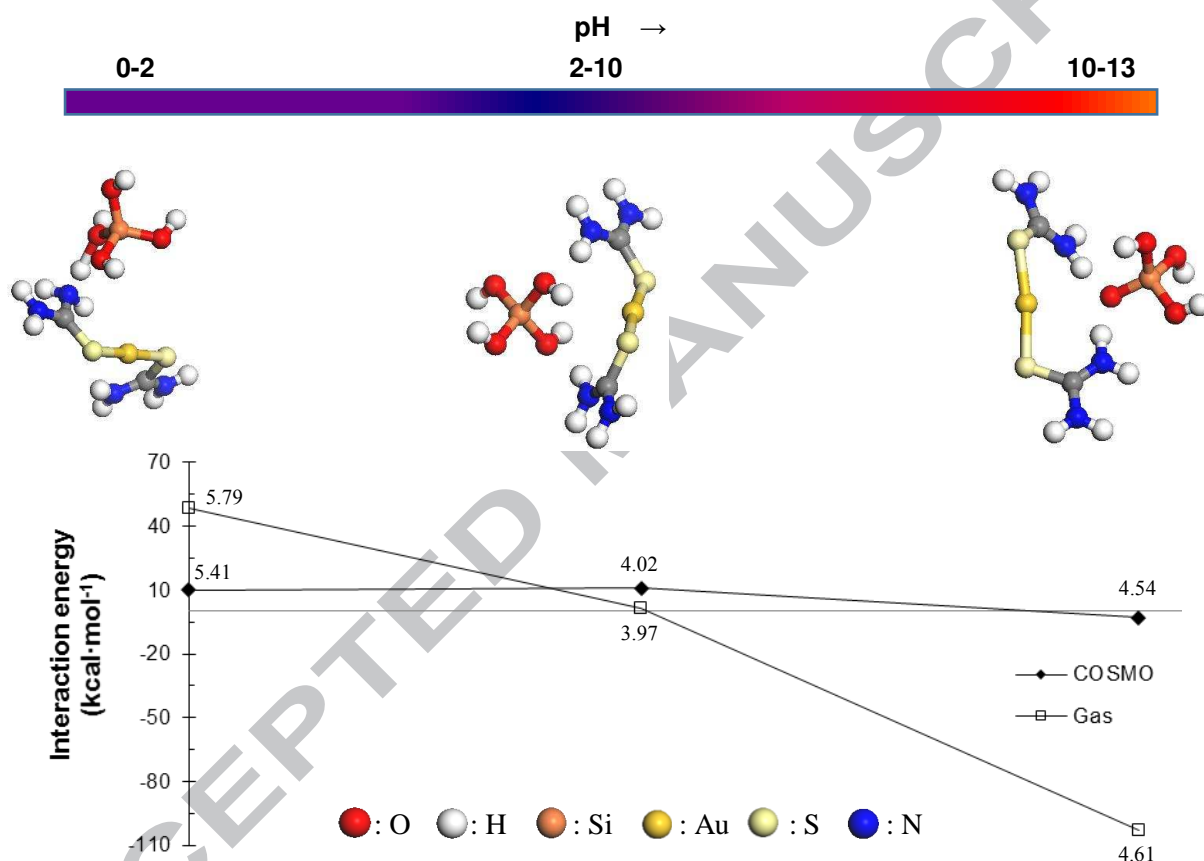
Figure 4. Optimised geometries of gold thiourea species interacting with different silica monomers in COSMO, and interaction energies calculated in both gas and COSMO. The values on each data point show the Au-Si distance in Å.

The gold thiourea cations and aqueous silica monomers in Figure 4 show a strong interaction in alkaline media, which correlates with experimental results [26]. The adsorption tests in thiourea media revealed a significant loss of gold in quartz-containing alkaline media (up to 0.1 µmol.m^{-2}) while in acidic media the adsorption was negligible. This is not surprising as an attractive force was expected between the opposite-charged ions present at higher pH, while the positive ions at lower pH

result in a repulsive force. The interaction energies calculated by the DFT method also replicate the experimental results at different pH values very well.

3.3.3. Thiosulphate System

Similar to gold thiourea, the interaction of gold thiosulphate with silica monomers including neutral $Si(OH)_4$, deprotonated $SiO(OH)_3^-$ at higher pH and protonated $Si(OH)_3(OH_2)^+$ at lower pH was investigated in both gas and COSMO phase. The optimised geometries as well as interaction energy are presented in Figure 5. The optimised geometries are based on COSMO models.
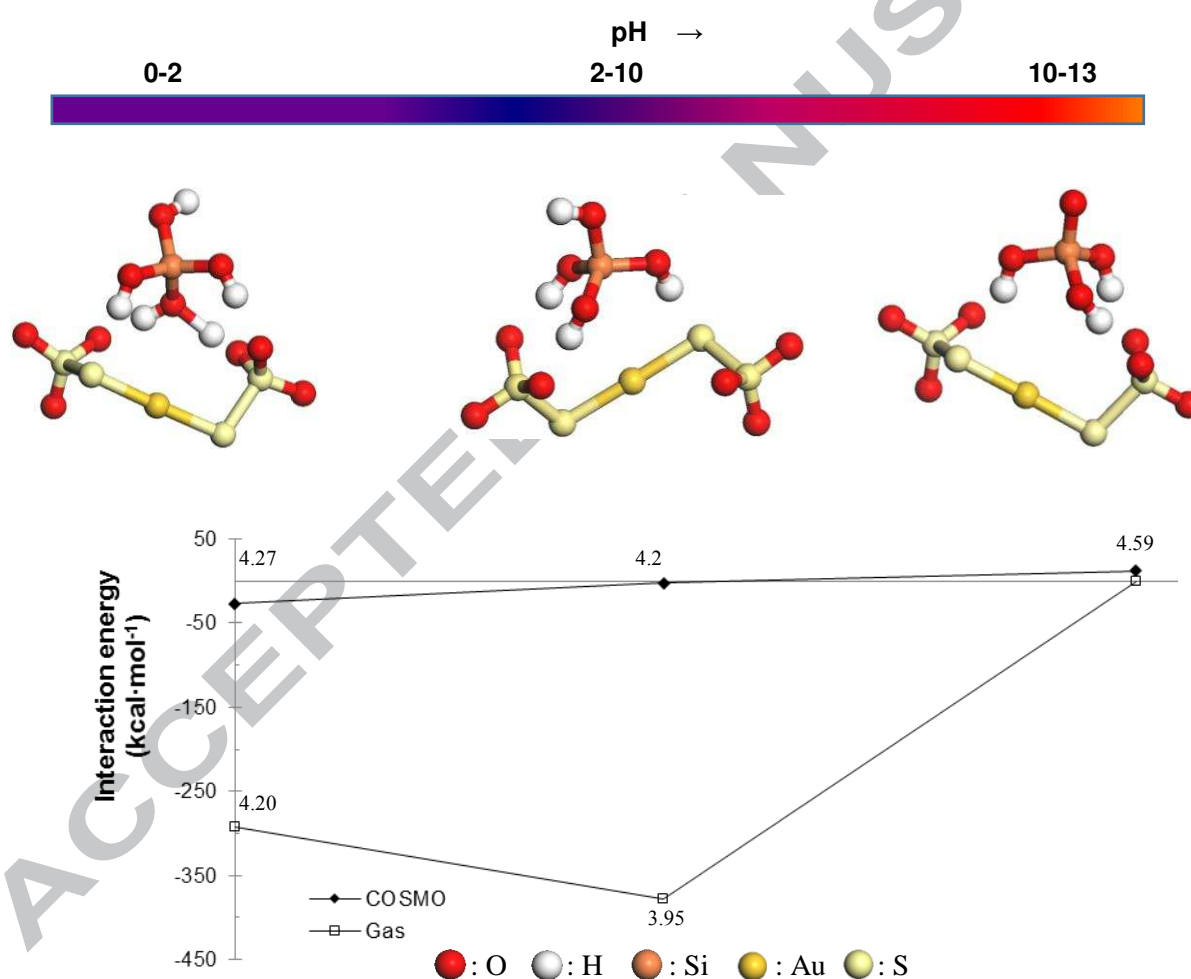

Figure 5. Optimised geometries of thiosulphate species and different silica monomers in COSMO and interaction energies in both gas and COSMO. The values on each data point show the Au-Si distance in Å.

The gold thiosulphate species show surprisingly strong interactions in the gas phase; the Gibbs energy is strongly negative for all monomers except the deprotonated silica. We also observed an

interesting effect in the gas phase reaction of deprotonated $Si(OH)_3O^-$ and gold thiosulphate. There is a strong repulsion between these two species, which is even effective at distances of more than 17 nm between the central ions of Si and Au in the two species during geometry optimisation. That is where the optimisation was stopped here, and the SCF energy of the interaction was converging to the sum of the individual molecules ($E_{Si\ monomer} + E_{AuTs}$) and thus the interaction energy tending to 0 as presented in Figure 5.

However, the effect of COSMO media results in much lower interaction energy, but still favourable for neutral $Si(OH)_4$ and deprotonated $Si(OH)_3(OH_2)^+$. At alkaline pH, the repulsive forces between similar ions, and the absence of any other positive ions to neutralise the surfaces, results in an unfavourable interaction. However, this is not the case at acidic pH, so gold loss due to adsorption by silica monomers does not seem to be a problem in thiosulphate media. This is in agreement with the experimental results in thiosulphate systems, which showed almost no gold adsorption onto clays and minimal adsorption onto framework silicates [26]. Some adsorption was observed for framework silicates, especially in feldspar, but this was attributed to the effect of cations present in the aqueous phase by dissolution of Al, Na, Ca and minor Fe from the feldspar minerals used.

3.4. COMPARISON BETWEEN INTERACTION ENERGIES

Figure 6 illustrates the complexes which are stable at different pH ranges used in the experimental studies presented in previous work [26], spanning the common pH ranges used in practical application (Table 4), along with interaction energies calculated from DFT modelling in COSMO media. The results obtained for gold preg-robbing by quartz (which has similar charging tendencies to the silica monomer) in the different systems reported in [26] are also depicted in Figure 6 as a function of pH for comparison. The correlation between the experimental and theoretical results is good. The strongest adsorption corresponds to alkaline thiourea and chloride systems, while the weakest adsorption occurs in acidic thiourea systems.

The comparison of theoretical and experimental results confirms the good agreement between results obtained by adsorption tests and calculated theoretical parameters based on optimised geometries in the DFT method. It also reveals the capability of the DFT method (DNP basis set, PBE exchange-correlation functionals, a 10 Å orbital cut off without pseudo-potentials or effective core potentials) to predict adsorption behaviour of aqueous ions through the use of appropriately selected small molecules to represent the surface chemistry and charge state, when the COSMO model is used to

represent the solvent contributions. This implicit solvation model is computationally efficient and can provide a reasonable description of the solvent behaviour comparable with experimental results.

This is highly beneficial in obtaining a better understanding of the parameters controlling the preg-robbing behaviour of silicates, which represents the first ever application of this calculation technique to the explanation of complex trends in gold hydrometallurgy.
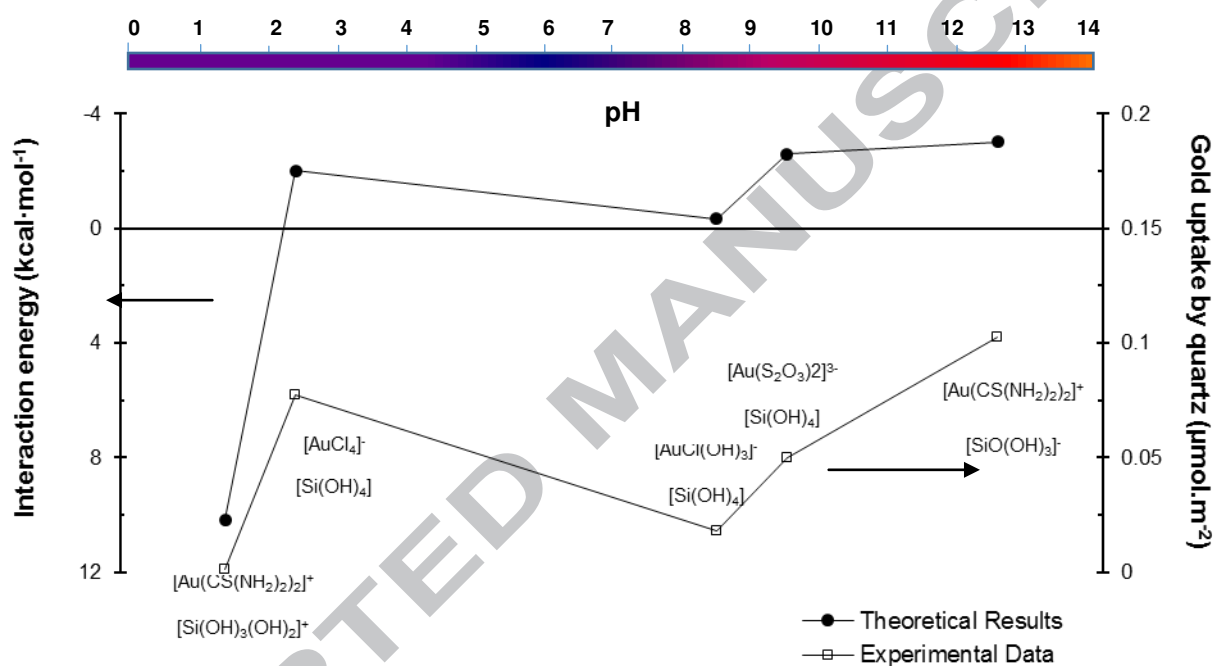
Figure 6. Gold and silica species identified in as stable under different pH conditions used in experiments, and the interaction energies of different silica monomers with different gold ligands based on experimental conditions.

4. CONCLUSIONS

The interaction energies of gold complexes with silica species based on theoretical studies are compared with the extent of silica preg-robbing results reported previously. The interaction energies computed using DFT and the COSMO model show satisfactory agreement with the amount of gold uptake per surface area of quartz.

The interaction of the gold chloro-hydroxy species with the silica monomer appeared to be unfavourable, except for $AuCl(OH)_3^-$ which is slightly favourable. The results are in agreement with

trends in gold preg-robbing by different silicates, especially quartz. The only controversy observed was related to $AuCl_4^-$ at pH 2.5-3, which indicated the dominant monomer is $Si(OH)_3(OH_2)^+$; the refined calculation using this protonated form of silica resulted in satisfactory agreement with the experimental results.

The interaction of gold thiourea and silica monomers shows that the adsorption is only effective at pH > 10, where deprotonation of silica monomers results in attractive electrostatic force between opposite ions. The interaction of gold thiosulphate with silica monomers at different pH values also showed favourable reactions for neutral $Si(OH)_4$ and deprotonated $Si(OH)_3(OH_2)^+$ monomers, while at alkaline pH the reaction is disfavoured. As gold thiosulphate is only stable at alkaline pH, gold loss via preg-robbing by silicates does not seem to be a problem in thiosulphate media.

The ability of DFT to compute the interactions of different gold complexes (including significant relativistic effects) with other species of industrial importance, has been demonstrated in this study. This allows us to explain and control the chemical processes which result in loss of gold from solution in hydrometallurgical extraction.

5. ACKNOWLEDGEMENTS

6. REFERENCES

[1]. J.D. Miller, R.Y. Wan, X. Díaz, Preg-robbing gold ores, in: Advances in Gold Ore Processing, M.D. Adams (Ed.) Elsevier, Amsterdam, 2005, pp. 937-972.

[2]. J. Gómez-Díaz, K. Honkala, N. López, A density functional theory study on gold cyanide interactions: The fundamentals of ore cleaning. Surf. Sci. 604 (2010) 1552-1557.

[3]. S. Mohammadnejad, J.L. Provis, J.S.J. van Deventer, The effect of grinding mechanism on the preg-robbing of gold onto quartz. Int. J. Miner. Proc. 128 (2014) 1-5.

[4]. S. Mohammadnejad, J.L. Provis, J.S.J. van Deventer, Effects of grinding on the preg-robbing behaviour of pyrophyllite. Hydrometall. 146 (2014) 154-163.

[5]. S. Mohammadnejad, J.L. Provis, J.S.J. van Deventer, Reduction of gold(III) chloride to gold(0) on silicate surfaces. J. Colloid Interf. Sci. 389(2013) 252-259.

[6]. S. Mohammadnejad, J.L. Provis, J.S.J. van Deventer, Effects of grinding on the preg-robbing potential of quartz in an acidic chloride medium. Miner. Eng. 52 (2013) 31-37.

[7]. S. Mohammadnejad, J.L. Provis, J.S.J. van Deventer, Gold sorption by silicates in acidic and alkaline chloride media. Int. J. Miner. Proc. 100 (2011) 149-156.

[8]. D. Feng, J.L. Provis, J.S.J. van Deventer, Adsorption of gold on albite in acidic chloride media. Hydrometall. 134–135 (2013) 32-39.

[9]. J.A. Tossell, The speciation of gold in aqueous solution: A theoretical study. Geochim. Cosmochim. Acta 60 (1996) 17-30.

[10]. U. Becker, M.F. Hochella Jr, D.J. Vaughan, The adsorption of gold to galena surfaces: Calculation of adsorption/reduction energies, reaction mechanisms, XPS spectra, and STM images. Geochim. Cosmochim. Acta 61 (1997) 3565-3585.

[11]. H. Hong, Z. Fu, X. Min, The adsorption of $[Au(HS)_2]^-$ on kaolinite surfaces: quantum chemistry calculations. Can. Miner. 39(2001) 1591-1596.

[12]. H. Hong, R. Xiao, X. Min, Reaction activity of kaolinite surfaces: quantum chemistry calculations. J. Wuhan Univ. Technol. - Mater. Sci. 18 (2003) 9-12.

[13]. A. Wojtaszek, I. Sobczak, M. Ziolek, F. Tielens, Gold grafted to mesoporous silica surfaces, a molecular picture. J. Phys. Chem. C 113 (2009) 13855-13859.

[14]. A. Wojtaszek, I. Sobczak, M. Ziolek, F. Tielens, The formation of gold clusters supported on mesoporous silica material surfaces: A molecular picture. J. Phys. Chem. C 114 (2010) 9002-9007.

[15]. S. Mohammadnejad, J.L. Provis, J.S.J. van Deventer, Computational modelling of gold complexes using density functional theory. Comput. Theor. Chem. 1073 (2015) 45-54.

[16]. B. Delley, From molecules to solids with the DMol3 approach. J. Chem. Phys. 113 (2000) 7756-7764.

[17]. P. Tréguer, D.M. Nelson, A.J. Van Bennekom, D.J. DeMaster, A. Leynaert, B. Quéguiner, The silica balance in the world ocean: a reestimate. Science 268 (1995) 375-379.

[18]. R.K. Iler, The Chemistry of Silica: Solubility, Polymerization, Colloid and Surface Properties and Biochemistry of Silica. John Wiley & Sons, New York, 1979.

[19]. H.E. Bergna, W.O. Roberts, Colloidal Silica: Fundamentals and Applications. Taylor & Francis, Boca Raton, 2005.

[20]. C.E. White, J.L. Provis, G.J. Kearley, D.P. Riley, J.S.J. van Deventer, Density functional modelling of silicate and aluminosilicate dimerisation solution chemistry. Dalton Trans. 40 (2011) 1348-1355.

[21]. M.J. Mora-Fonz, C.R.A. Catlow, D.W. Lewis, Modeling aqueous silica chemistry in alkali media. J. Phys. Chem. C 111 (2007) 18155-18158.

[22]. J.A. Tossell, N. Sahai, Calculating the acidity of silanols and related oxyacids in aqueous solution. Geochim. Cosmochim. Acta 64 (2000) 4097-4113.

[23]. P.W. Schindler, W. Stumm, The surface chemistry of oxides, hydroxides, and oxide minerals, in: Aquatic Surface Chemistry: Chemical Processes at the Particle-Water Interface, W. Stumm (Ed), Wiley, New York, 1987, pp. 83-110.

[24]. J. Šefčík, W.A. Goddard III, Thermochemistry of silicic acid deprotonation: comparison of gas-phase and solvated DFT calculations to experiment. Geochim. Cosmochim. Acta 65 (2001) 4435-4443.

[25]. F. Moreau, G.C. Bond, A.O. Taylor, Gold on titania catalysts for the oxidation of carbon monoxide: control of pH during preparation with various gold contents. J. Catal. 231 (2005) 105-114.

[26]. S. Mohammadnejad, The role of silicates in gold processing, Ph.D. thesis, The University of Melbourne, 2014. 159 pp.

Graphical abstract
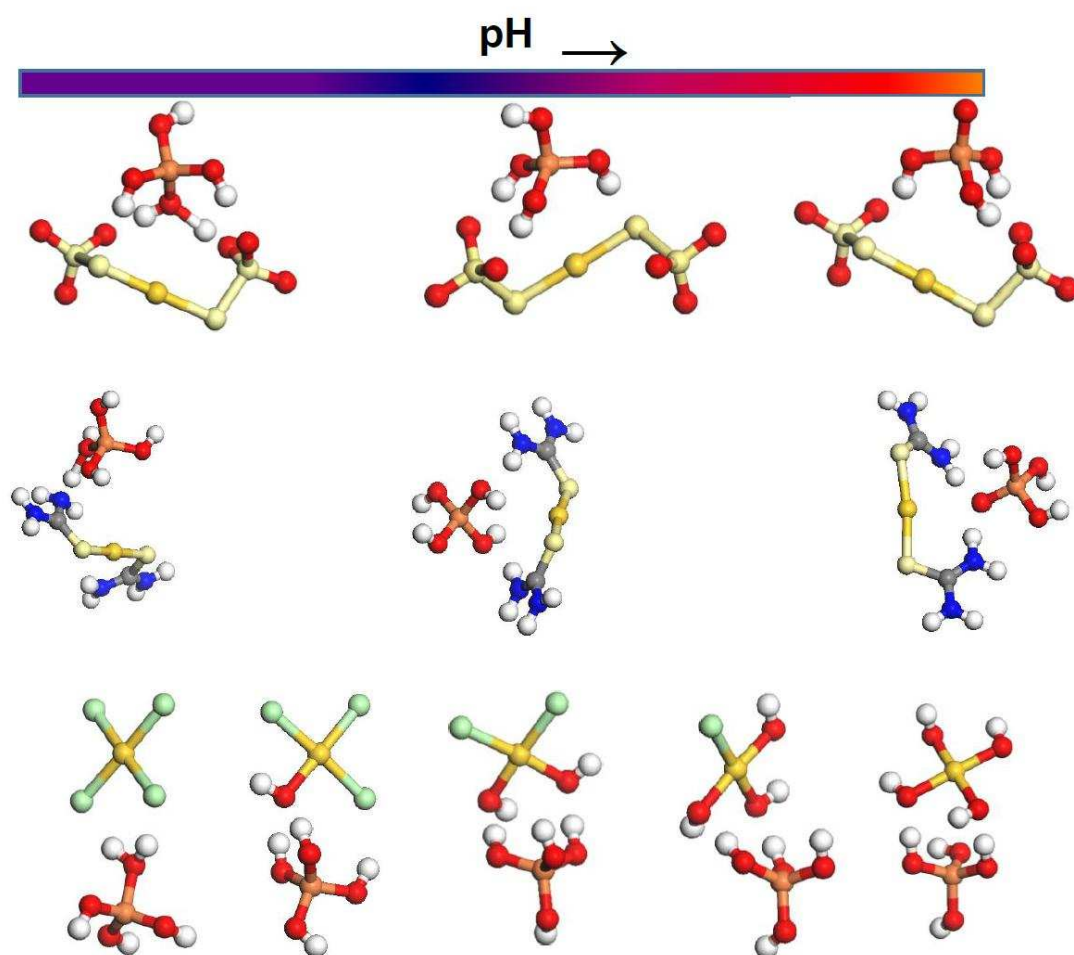
Highlights

- Interactions of gold complexes with silicates described by DFT simulation

- COSMO model enables reproduction of macroscopic experimental data

- Provides a new theoretical description of silicate preg-robbing